Particles Separation and Tracks in a Hydrocyclone

Chih-Yuan Hsu[1], Syuan-Jhih Wu[1] and Rome-Ming Wu[1,2]*

[1]*Department of Chemical and Materials Engineering, Tamkang University, Tamsui, Taiwan 251, R.O.C.*
[2]*Energy and Opto-Electronic Materials Research Center, Tamkang University, Tamsui, Taiwan 251, R.O.C.*

Abstract

Hydrocyclone separation technique recently has been used in an increasing number of applications. Reynolds Stress Turbulence Model (RSM) and Discrete Phase Model (DPM) were employed in Computational Fluid Dynamics (CFD) 3D simulation to draw the motion trace of single particle of different particle size and density in hydrocyclone separator. It is known that, smaller size particles flow out from overflow, larger size particles flow out from underflow, and there is a characteristic size of particles having longer residence time in hydrocyclone separator. Particle size influences separation efficiency more significantly than particle density. Simulation of particle cluster separation efficiency in hydrocyclone separator has some discrepancy from experimental result. It is because air core influence is not considered in this study.

***Key Words*:** Hydrocyclone, CFD, DPM, RSM

1. Introduction

Hydrocyclones have been used for mineral processing for more than 100 years. Nowadays hydrocyclones are extensively used in the industry to remove or classify particles, and to separate particles by density or size [1–5]. Hydraulic residence times for hydrocyclones are about 1–2 s, compared to several minutes for traditional gravity separators [6]. The fluid flows into hydrocyclone and develops an outer vortex and a reversed inner vortex, where particles move in the underflow and in the overflow direction, respectively. In such vortex systems centrifugal fields as strong as 2000–3000 g are created [7]. Therefore an air core forms due to high centrifugal forces and an open overflow [8]. The air core in hydrocyclone will arise turbulence fluctuation, and decrease separation efficiency [9].

The velocity profiles of hydrocyclones were first measured by Kelsall [10], he found that the tangential velocity increased to a maximum from hydrocyclone wall towards the center, and then decreased rapidly. Some studies agree on the same qualitative flow behavior [11,12]. Owing to a strong air core in the center, tangential and axial velocities become difficult to measure. However, with the development of science and technology, researchers focus on simulations by Computational Fluid Dynamics (CFD) techniques [13].

The first work in predicting the fluid flow in hydrocyclones was successfully achieved by Pericleous and Rhodes [14]. They applied the improved Prandtl mixing length model to simulate the hydrocyclone separator of 200-mm diameter, and compared the velocity distribution acquired with Laser Doppler Velocimeter (LDV) measured velocity distribution. Later, Hsieh and Rajamani [15] solved the equation of turbulent flow motion, and compared the solutions with LDV measured flow pattern of 75-mm hydrocyclone separator.

Recently, Medronho et al. [16] used CFD studies to simulate the separation of microorganisms and mammalian cells with hydrocyclones. Some works on the simulation of hydrocyclones using the incompressible Navier-Stokes equations, supplemented by a suitable

*Corresponding author. E-mail: romeman@mail.tku.edu.tw

turbulence model, have proven to be appropriate for modeling the flow in a hydrocyclone [17,18]. Xu et al. [19] investigated numerical methods for simulating a hydrocyclone, including RNG k-ε, RSM, LES etc. They concluded that RNG k-ε is not suitable for modeling hydrocyclone, while the performances of RSM and LES models are close to each other and the experimental results.

A CFD study is presented for the calculation of the three-dimensional flow and separation efficiency for particles with low concentrations in a hydrocyclone. The particles tracks and flow pattern of a hydrocyclone were compared with experimental results.

2. Numerical Methods

2.1 Geometry and Meshes

The geometry of the hydrocyclone is displayed in Figure 1. The diameters of feed, overflow, underflow, and hydrocyclone are 8, 10, 5, and 30 mm, respectively. The length of the cylindrical part is 65 mm, while the length of the cone part is 75 mm, making an overall 19° cone angle.

A grid independence study was carried out with three different mesh densities with mesh sizes varying from 50,000, 75,000 to 250,000. A mesh density of 75,000 cells was optimal for good simulations and reasonable computational time and was shown as Figure 2.

2.2 Water Flow and Turbulence Model

The simulation of the high-turbulent flow in hydrocyclone requires the basic equations of fluid dynamics combined with an adequate turbulence model. The flow pattern in hydrocyclone was modeled by Newtonian water flow and by Reynolds Stress turbulence Model (RSM). The Reynolds-averagred Navier-Stokes equations are described as follows:

$$\frac{\partial \rho}{\partial t} + \frac{\partial \rho}{\partial x_i}(\rho v_i) = 0 \quad (1)$$

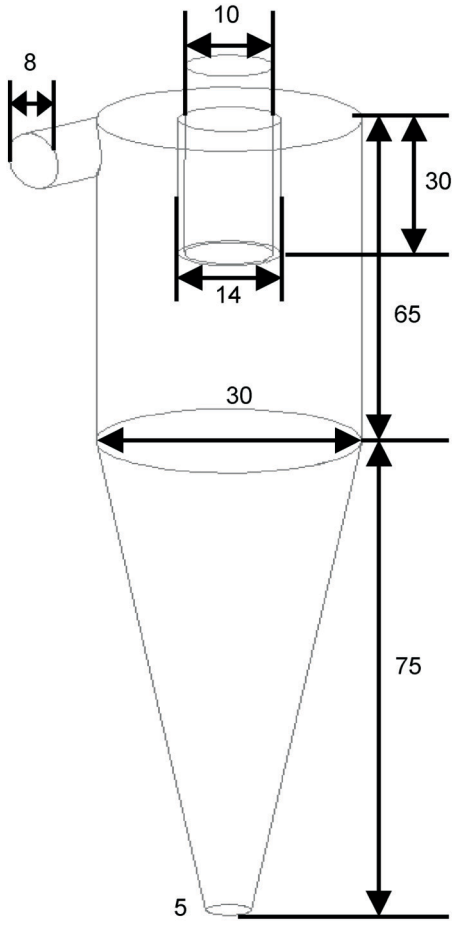

Figure 1. Geometry of the 30-mm hydrocyclone.

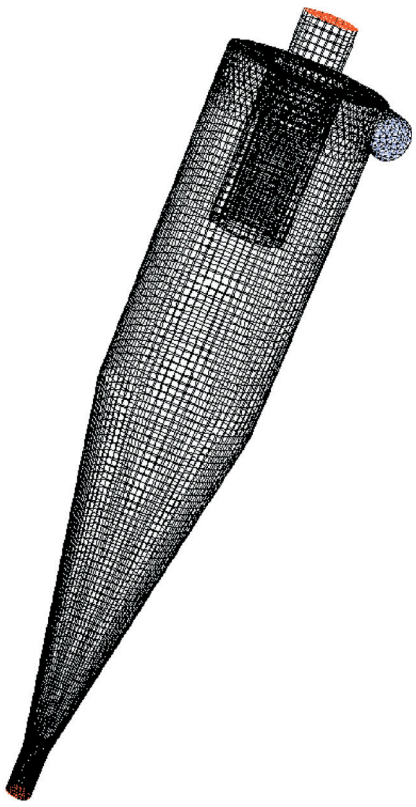

Figure 2. Meshes of the hydrocyclone.

$$\frac{\partial}{\partial t}(\rho v_i)+\frac{\partial}{\partial x_j}(\rho v_i v_j)=-\frac{\partial p}{\partial x_i}$$
$$+\frac{\partial}{\partial x_j}[\mu(\frac{\partial v_i}{\partial x_j}+\frac{\partial v_j}{\partial x_i}-\frac{2}{3}\delta_{ij}\frac{\partial v_j}{\partial x_j})]+\frac{\partial}{\partial x_j}(-\rho\overline{v_i'v_j'}) \quad (2)$$

The exact transport equations for the transport of the Reynolds stresses, $\rho\overline{v_t'v_j'}$, may be written as follows:

$$\frac{\partial}{\partial t}(\rho\overline{v_i'v_j'})+\frac{\partial}{\partial x_k}(\rho v_k\rho\overline{v_i'v_j'})=-\frac{\partial}{\partial x_k}[\rho\overline{v_i'v_j'v_k'}+\overline{p(\delta_{kj}v_i'+\delta_{ik}v_j')}]$$
$$+\frac{\partial}{\partial x_k}[\mu\frac{\partial\overline{v_i'v_j'}}{\partial x_k}]-\rho(\overline{v_i'v_j'}\frac{\partial v_j}{\partial x_k}+\overline{v_j'v_k'}\frac{\partial v_i}{\partial x_k})-\rho\beta(g_i\overline{v_j'\theta}+g_j\overline{v_i'\theta})$$
$$+\overline{p(\frac{\partial v_i'}{\partial x_j}+\frac{\partial v_j'}{\partial x_i})}-2\mu\overline{\frac{\partial v_i'}{\partial x_k}\frac{\partial v_j'}{\partial x_k}} \quad (3)$$

where the left-hand side are local time derivative and convection terms, The right-hand side are turbulent diffusion, molecular diffusion, stress production, buoyancy production, pressure strain, and dissipation terms, respectively.

2.3 Boundary Conditions

A velocity inlet boundary condition was applied at the inlet:

$$\vec{u}=const. \quad @ \text{ inlet pipe} \quad (4)$$

The overflow and underflow used pressure outlet boundary conditions. The outlet fluid is moving under absolute pressure 1 atm therefore the gauge pressure at the overflow and underflow are zero. The boundary conditions are:

$$P=0 \quad @ \text{ underflow} \quad (5)$$

$$P=0 \quad @ \text{ overflow} \quad (6)$$

The computational fluid dynamics program FLUENT 6.2 (Fluent Inc., USA) solved the governing equations, Eqns. (1)–(3), together with the associated boundary conditions Eqns. (4)–(6).

The pressure staggered option (PRESTO), which is a pressure interpolation scheme reported as useful for predicting the high swirl flow characteristics that prevail inside the hydrocyclone body, was adopted. The SIMPLE algorithm scheme, which uses a combination of continuity and momentum equations to derive an equation for pressure, was applied. Simulations were carried out for about 50,000 incremental steps where in general a preset value of convergence criteria 1×10^{-4} was achieved.

2.4 Discrete Particle Model

The dispersion of particles due to turbulence can be predicted using the stochastic tracking model, which includes the effect of instantaneous turbulent velocity fluctuations on the particle trajectory. FLUENT predicts the trajectory of a discrete phase particle by integrating the force balance on the particle. This force balance can be written as (for x direction):

$$\frac{du_p}{dt}=F_D(u-u_p)+\frac{g_x(\rho_p-\rho)}{\rho_p} \quad (7)$$

where $F_D(u-u_p)$ is the drag force per unit particle mass and

$$F_D=\frac{18\mu}{\rho_p d_p^2}\frac{C_D\,\mathrm{Re}}{24} \quad (8)$$

where u is the fluid phase velocity, u_p is the particle velocity, μ is the molecular viscosity of the fluid, ρ is the fluid density, ρ_p is the density of the particle, and d_p is the particle diameter. Re is the relative Reynolds number, which is defined as

$$\mathrm{Re}=\frac{\rho d_p|u_p-u|}{\mu} \quad (9)$$

3. Experiments

Potato starch powders with average diameter 47.4 μm and density density 1450 kg/m^3 were used as sample particles. Particle size distribution analyses of samples and underflow/overflow received in collection tanks were carried out using Coulter LS 230, a device working on Laser diffraction principles. The parameters used in the simulation are the same with experiments and listed in Table 1.

Figure 3 shows all devices for experiment, including pump, tank, agitator, pressure gauge and hydrocyclone separator. The liquid is pumped to the cyclone by a cen-

Table 1. Parameters in the experiment and simulation

Operating Pressure (bar)	0.5	1.0	1.5	2.0
Inlet velocity (m/s)	0.04	0.05	0.07	0.08
Particle density (kg/m^3)		1450		
Volume percentage (%)		3.62		

trifugal pump (P). There is a gate valve (V1) between the tank and the centrifugal pump. The volumetric flow rate of feed slurry can be maintained by regulating the flow through a gate valve (V1) between tank and centrifugal pump and by regulating the gate valve (V2) through the bypass line. The flow through apex and split chamber can be controlled by valve (V3) and valve (V4).

4. Results and Discussion

4.1 Performance of the Hydrocyclone

The parameters used in this study are the same with experiments and listed in Table 1. Grad-efficiency curves are obtained by means of a stochastic particle tracking technique and shown as Figure 4.

The larger the operation pressure, the higher the efficiency curve, which indicates that the more possibility small particles flow out through underflow.

As shown in Figure 4, fish hook effect can be clearly observed in experimental result, 17.4 μm particle has the lowest separation efficiency. Simulation has similar result (18.2 μm). As to larger particle size (> 30 μm), experiment result fits in with simulation generally. Small particle size part (< 30 μm) can be further divided into 2 intervals, 6–30 μm particles flow out from underflow more easily in simulation than in practice, while < 6 μm particles flow out from underflow not so easily in simulation than in practice. In experiment, there is a steady, cylindrical-like air core formed in the center of hydrocyclone. Such differences between experiments and simulations might be because air core impact is not considered in simulation.

Though there still has difference compared with experimental data, the authors believe the methods in this study is a good tool to investigate hydrocyclone. In order to eliminate effect of particle-particle interaction, single particle injection and particle track in a hydrocyclone is discussed below.

4.2 Particle Track in a Hydrocyclone

In Figure 5, simulation method is used to track trace

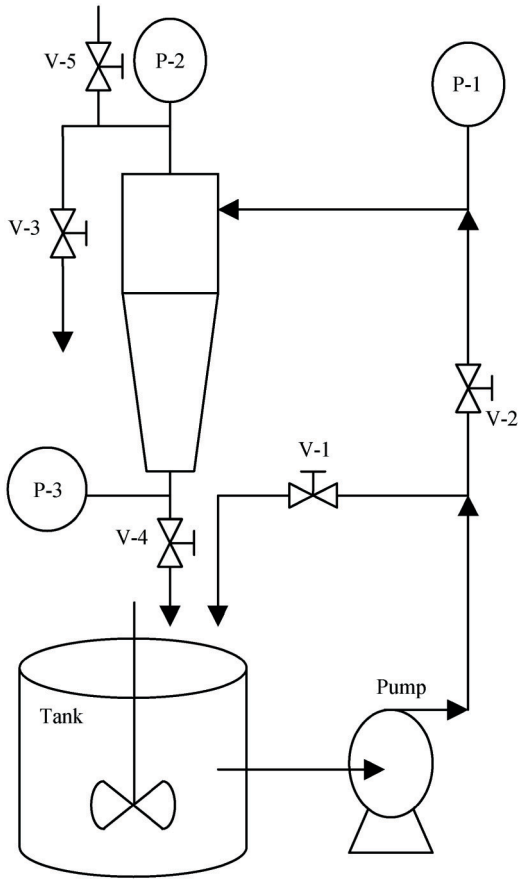

Figure 3. Experiment setup.

and residence time of single particle of different particle size and density in hydrocyclone separator. As shown in Figures 5(a), (b), (c), when particle size is smaller (10 μm), particles of three densities flow out from overflow, residence time is 0.56 s, 0.57 s, and 0.61 s respectively. With greater density, the residence time is longer. Moreover, particle flowing scope is confined in the upper half of hydrocyclone separator-cylinder part.

As shown in Figures 5(d), (e), (f), when particle size increases to 100 μm, particles of three densities flow out from underflow, residence time is 0.84 s, 0.78 s, and 0.77 s respectively. With greater density, the residence time is shorter. Moreover, particles flow directly from upper cylindrical part of hydrocyclone to lower cone part.

As shown in Figures 5(g), (h), (i), when particle size is a characteristic value, d_c, the residence time is the longest among the same kind of particles, e.g., for 1500 kg/m^3 particle, d_c is 25 μm, residence time is 1.15 s; for 3000 kg/m^3 particle, d_c is 13 μm, residence time is 1.34 s. The greater the density, the smaller the characteristic

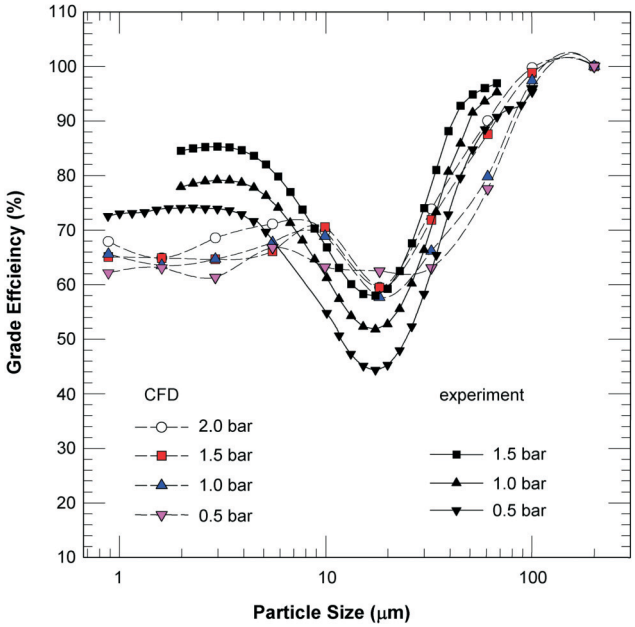

Figure 4. Grad-efficiency curves.

particle size d_c, and the longer the residence time.

In Figures 5(g), (h), (i), particles flow downward to lower cone part of hydrocyclone, then flow upward to upper cylindrical part of hydrocyclone, leading to longer residence time, hence, proper design of joint of upper cylinder and lower cone of hydrocyclone separator may improve separation efficiency.

5. Conclusion

The total separation efficiency obtained from DPM still had a disparity when compared with experiment. Improvements for hydrocyclone to obtain a smaller characteristic size, d_c, have continuously been studied. An increased knowledge of how a certain change of the flow field influences the overall separation process would be of great benefit for the continued development of hydrocyclones.

The residence time of particles in a hydrocyclone is longest for certain characteristic particle size, and density variation influence on such characteristic particle size is insignificant. Particle size influences separation efficiency more significantly than particle density.

Nomenclature

C_D drag coefficient, -

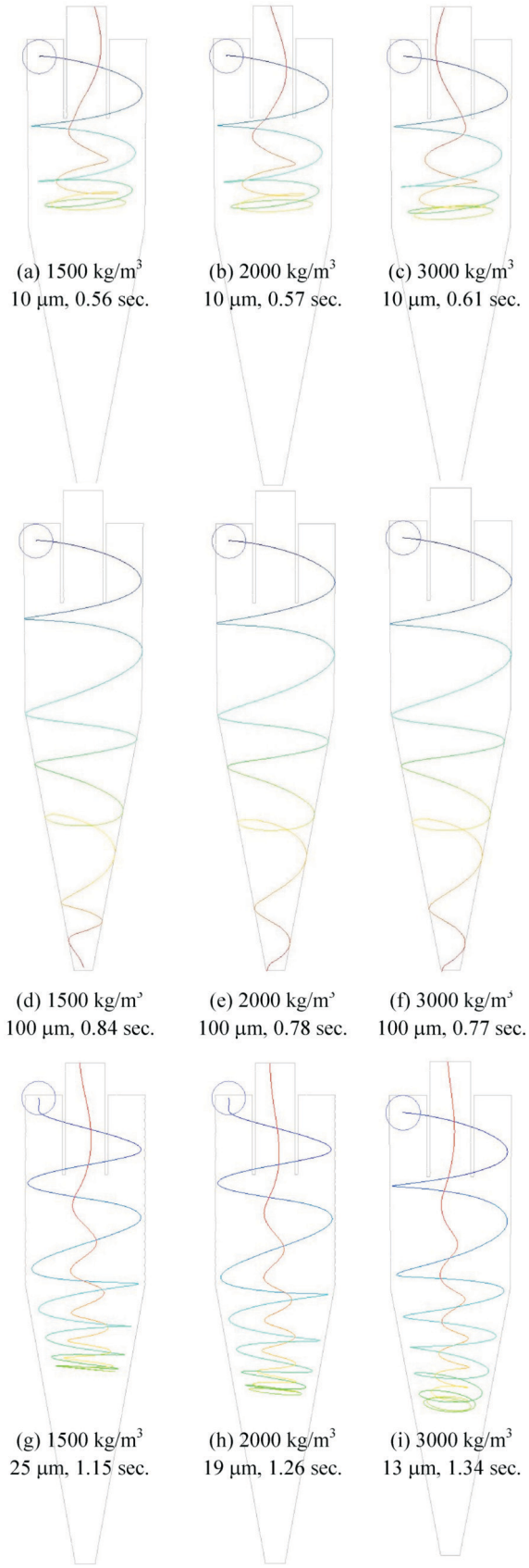

Figure 5. Particles tracks.

d_c characteristic size, m
d_p diameter of particle, m
F_D drag force, N
P pressure, N/m^2
u velocity of fluid, m/s
u_p velocity of particle, m/s
μ viscosity of fluid, kg/m-s
ρ density of fluid, kg/m^3
ρ_p density of particle, kg/m^3

Acknowledgements

The authors would like to acknowledge the financial support received from the National Science Council of Republic of China.

References

[1] Yoshioka, N. and Hotta, Y., "Liquid Cyclone as a Hydraulic Classifier," *J Chem Eng Japan*, Vol. 19, pp. 632–640 (1955).

[2] Trim, D. S. and Marder, R. C., "Investigations of Hydrocyclones for Concentration of Cassava Milk," *Starch-Starke*, Vol. 47, pp. 306–311 (1995).

[3] Klimpel, R. R., "The Influence of Chemical Dispersant on the Sizing Performance of a 24-in Hydrocyclone," *Powder Technol*., Vol. 31, pp. 255–262 (1982).

[4] Dyakowski, T. and Williams, R. A., "Modelling Turbulent Flow within a Small-Diameter Hydrocyclone," *Chem Eng Sci*., Vol. 48, pp. 1143–1152 (1993).

[5] Yuan, H. D., Rickwood, T. C. S. and Thew, M. T., "An Investigation into the Possible Use of Hydrocyclones for the Removal of Yeast from Beer," *Bioseparation*, Vol. 6, pp. 159–163 (1996).

[6] Thew, M. T. and Smyth, I. C., "Development and Performance of Oil-Water Hydrocyclone Separators – A Review," In: *Innovation in Physical Separation Technologies*, Pub. The Institution of Mining and Metallurgy, London, pp. 77–89 (1998).

[7] Sinker, A. B., Humphris, M. and Wayth, N., "Enhanced Deoiling Hydrocyclone Performance without Resorting to Chemicals," In: *Paper SPE 56969 Presented at the Offshore Europe Conference*, Aberdeen, Scotland (1999).

[8] Wanwilai, K. E., Anotai, S. and Andrzej, F. N., "The Simulation of the Flow within a Hydrocyclone Operating with an Air Core and with an Inserted Metal Rod," *Chem Eng J*., Vol. 143, pp. 51–61 (2008).

[9] Sripriya, R., Kaulaskar, M. D., Chakraborty, S. and Meikap, B. C., "Studies on the Performance of a Hydrocyclone and Modeling for Flow Characterization in Presence and Absence of Air Core," *Chem Eng Sci*., Vol. 62, pp. 6391–6402 (2007).

[10] Kelsall, D. F., "A Study of the Motion of Solid Particles in a Hydraulic Cyclone," *Trans Instn Chem Engrs*., Vol. 30, pp. 87–108 (1952).

[11] Bergstrom, J. and Vomhoff, H., "Experimental Hydrocyclone Flow Field Studies," *Sep Purif Tech*., Vol. 53, pp. 8–20 (2007).

[12] Bergstrom, J., Vomhoff, H. and Soderberg, D., "Tangential Velocity Measurements in a Conical Hydrocyclone Operated with a Fibre Suspension," *Minerals Eng*., Vol. 20, pp. 407–413 (2007).

[13] Hsu, C. Y. and Wu, R. M., "Hot Zone in a Hydrocyclone for Particles Escape from Overflow," *Dry Tech*., Vol. 26, pp. 1011–1017 (2008).

[14] Pericleous, K. A. and Rhodes, N., "The Hydrocyclone Classifier – A Numerical Approach," *Int J Mineral Process*, Vol. 17, pp. 23–43 (1986).

[15] Hsieh, K. T. and Rajamani, R. K., "Mathematical Model of the Hydrocyclone Based on Physics of Fluid Flow," *Am Institute Chem Eng J*., Vol. 37, pp. 735–746 (1991).

[16] Medronho, R. A., Schuetze, J. and Deckwer, W. D., "Numerical Simulation of Hydrocyclones for Cell Separation," *Lat Am Appl Res*., Vol. 35, pp. 1–8 (2005).

[17] Wang, B., Chu, K. W. and Yu, A. B., "Numerical Study of Particle-Fluid Flow in a Hydrocyclone," *Ind Eng Chem Res*., Vol. 46, pp. 4695–4705 (2007).

[18] Wang, B. and Yu, A. B., "Numerical Study of the Gas-Liquid-Solid Flow in Hydrocyclones with Different Configuration of Vortex Finder," *Chem Eng J*., Vol. 135, pp. 33–42 (2008).

[19] Xu, P., Wu, Z., Mujumdar, A. S. and Yu, A. B., "Innovative Hydrocyclone Inlet Designs to Reduce Erosion-Induced Wear in Mineral Dewatering Processes," *Drying Tech*., Vol. 27, pp. 201–211 (2009).

Manuscript Received: Sep. 26, 2009
Accepted: Sep. 6, 2010